

Written: August 1969

Distributed: March 10, 1970

LA-4245-MS
UC-34, PHYSICS
TID-4500

LOS ALAMOS SCIENTIFIC LABORATORY
of the
University of California
LOS ALAMOS • NEW MEXICO

Early Radio Flash from a
Low-Altitude Air Burst

by

B. R. Suydam



EARLY RADIO FLASH FROM
A LOW-ALTITUDE AIR BURST

by

B. R. Suydam

ABSTRACT

This report reworks an earlier theory of the early part of the radio flash from a low air burst by extending the results to quite general gamma ray vs. time histories, and to times about ten times longer than the earlier theory. The previous theory is also improved in that error estimates are given for all approximations used. Typical signal shapes are presented.

I. INTRODUCTION

Some time ago a method, called the high-frequency approximation, was developed for calculating, analytically, the early part of the radio flash from an air burst.⁽¹⁾ Subsequently the method was extended to a ground burst.⁽²⁾ The first of these references, however, suffers from two defects, namely: (1) it is classified, and (2) in it many approximations were made in order to obtain simple results without any estimates as to the limits of validity of the approximations. It has accordingly been deemed advisable to rework the theory removing as far as possible the defects.

Our analytical theory of the radio flash requires three classes of approximations:

1. Analytical approximations to the temporal and spatial behavior of the source functions, J and σ .
2. An approximate treatment of Maxwell's equations, arrived at by dropping certain troublesome terms.

3. The evaluation of certain integrals which express the solution of the simplified set of Maxwell's equations.

In Section II we derive the equations of the high-frequency approximation, first in full generality, and then specialized to the low-altitude air burst. In Section III we discuss the source functions J and σ in sufficient detail to indicate that the analytic form we assume is sufficiently general to cover all practical cases. Thus item 1. above presents no problem. In Section III we also calculate the radial E-field which is needed in the next section.

Section IV contains our results, namely analytic expressions for the radiated signal, together with typical curves. These results are, of course, based on our high-frequency approximation. This approximation may be viewed as the first term of a series expansion of the solution to Maxwell's equations. We have made the usual heuristic estimate of the limitations of the theory by calculating the second term of this expansion and noting under

what conditions it is negligibly small. The details of this calculation are in Appendix D. Generally speaking, we can be confident in the first microsecond of the calculated pulse. In order to express the solutions to our equations in simple closed form approximate expressions must be found for certain integrals. These approximations, together with remainder terms, are worked out in Appendices A and B. As the remainder terms given are exact, there can be no question as to the range of validity of our approximations; at the expense of more complicated formulas, correction terms of any desired precision can be added to our formulae.

Finally in Section V we discuss our results. In this section it is pointed out why one may ignore all nonlinear effects, as we have done throughout this work.

II. THE HIGH-FREQUENCY APPROXIMATION

The Compton current, J , and the electrical conductivity, σ , are both produced by a short pulse of gamma radiation which expands radially outward from the burst point with the speed of light. It is therefore appropriate to describe events in terms of proper time, τ , rather than ordinary time, t

$$(2.1) \quad \tau = t - r/c,$$

where r is distance from the burst point. When expressed in terms of proper time, τ , and position, r , the Compton current and the conductivity have approximately the forms

$$(2.2) \quad \begin{cases} J = j(r) f(\tau) \\ \sigma = s(r) g(\tau) \end{cases},$$

where f and g represent extremely short pulses. Clearly,

$$(2.3) \quad \frac{\partial J}{\partial r} \approx -J/\lambda \quad \text{and} \quad \frac{\partial \sigma}{\partial r} \approx -\sigma/\lambda.$$

where λ is the gamma-ray mean-free-path. Now λ/c is about $2/3$ microsecond and the pulses, f and g , are considerably narrower than this. Therefore the operator, $\partial/\partial r$, operating on J or σ , is much smaller than the

operator, $\partial/\partial \tau$. It is reasonable to assume that the same is true of the field quantities, at least for the early part of the signal. The high-frequency approximation consists in ignoring $\partial/\partial r$ of various field quantities compared with $\partial/\partial \tau$ of the same quantity. The dropping of such small terms must, however, be done with circumspection, first noting all cancellation that may exist among large terms before small ones are dropped.

The easiest way to see how the high-frequency approximation works in detail is to write out the full set of Maxwell's equations in polar coordinates, (r, θ, ϕ) , and in terms of the proper time, τ , rather than ordinary time, t . Under this transformation, Maxwell's equations take the form

$$(2.4) \quad \left\{ \begin{aligned} \frac{1}{c} \frac{\partial E_r}{\partial \tau} + 4\pi\sigma E_r &= -4\pi J_r + \frac{1}{r \sin \theta} \left[\frac{\partial(\sin \theta B_\phi)}{\partial \theta} - \frac{\partial B_\theta}{\partial \phi} \right], \\ \frac{1}{c} \frac{\partial E_\theta}{\partial \tau} + 4\pi\sigma E_\theta &= -4\pi J_\theta + \frac{1}{r \sin \theta} \frac{\partial B_r}{\partial \phi} \\ &\quad - \frac{1}{r} \frac{\partial(r B_\phi)}{\partial r} + \frac{1}{c} \frac{\partial B_\phi}{\partial \tau}, \\ \frac{1}{c} \frac{\partial E_\phi}{\partial \tau} + 4\pi\sigma E_\phi &= -4\pi J_\phi - \frac{1}{r} \frac{\partial B_r}{\partial \theta} + \frac{1}{r} \frac{\partial(r B_\theta)}{\partial r} \\ &\quad - \frac{1}{c} \frac{\partial B_\theta}{\partial \tau}, \\ \frac{1}{c} \frac{\partial B_r}{\partial \tau} &= \frac{1}{r \sin \theta} \left[\frac{\partial E_\theta}{\partial \phi} - \frac{\partial(\sin \theta E_\phi)}{\partial \theta} \right], \\ \frac{1}{c} \frac{\partial B_\theta}{\partial \tau} &= \frac{1}{r} \frac{\partial(r E_\phi)}{\partial r} - \frac{1}{r \sin \theta} \frac{\partial E_r}{\partial \phi} - \frac{1}{c} \frac{\partial E_\phi}{\partial \tau}, \\ \frac{1}{c} \frac{\partial B_\phi}{\partial \tau} &= \frac{1}{r} \frac{\partial E_r}{\partial \theta} - \frac{1}{r} \frac{\partial(r E_\theta)}{\partial r} + \frac{1}{c} \frac{\partial E_\theta}{\partial \tau}. \end{aligned} \right.$$

The first step is to eliminate B_θ and B_ϕ by formally integrating the last two equations

$$(2.5) \left\{ \begin{array}{l} rB_{\theta} = -rE_{\varphi} + \frac{\partial}{\partial r} \int_{-\infty}^{\tau} rE_{\varphi} c d\tau \\ - \frac{1}{\sin \theta} \frac{\partial}{\partial \varphi} \int_{-\infty}^{\tau} E_r c d\tau, \\ rB_{\varphi} = rE_{\theta} + \frac{\partial}{\partial \theta} \int_{-\infty}^{\tau} E_r c d\tau - \frac{\partial}{\partial r} \int_{-\infty}^{\tau} rE_{\theta} c d\tau. \end{array} \right.$$

Then substituting these results into the two equations for E_{θ} and E_{φ} gives

$$(2.6) \quad \frac{\partial}{\partial r} (rE_{\theta}) + 2\pi\sigma(rE_{\theta}) = -2\pi rJ_{\theta} + \frac{1}{2} \frac{\partial E_r}{\partial \varphi} \\ + \frac{1}{2 \sin^2 \theta} \frac{\partial B_r}{\partial \varphi} - \frac{1}{2} \frac{\partial^2}{\partial r \partial \theta} \int_{-\infty}^{\tau} E_r c d\tau + \frac{1}{2} \frac{\partial^2}{\partial r^2} \int_{-\infty}^{\tau} rE_{\theta} c d\tau$$

and

$$(2.7) \quad \frac{\partial}{\partial r} (rE_{\varphi}) + 2\pi\sigma(rE_{\varphi}) = -2\pi rJ_{\varphi} + \frac{1}{2 \sin \theta} \frac{\partial E_r}{\partial \varphi} \\ - \frac{1}{2} \frac{\partial B_r}{\partial \theta} - \frac{1}{2} \frac{1}{\sin^2 \theta} \frac{\partial^2}{\partial r \partial \varphi} \int_{-\infty}^{\tau} E_r c d\tau + \frac{1}{2} \frac{\partial^2}{\partial r^2} \int_{-\infty}^{\tau} rE_{\varphi} c d\tau.$$

So far everything is exact; Eqs. (2.5), (2.6) and (2.7) together with the first and fourth of Eqs. (2.4) are equivalent to the original Maxwell equations. Note that in Eqs. (2.6) and (2.7) the cancellation of the two large radiation terms has taken place.

The high-frequency approximation consists now in taking the awkward set of equations (2.5), (2.6) and (2.7) and ignoring terms in $\partial/\partial r$, as compared with those in $\partial/c d\tau$ of the same quantity. Consider, for example, the first two terms on the right-hand side of Eq. (2.5). We see that

$$(2.8) \quad rE_{\varphi} = \frac{\partial}{c \partial \tau} \int_{-\infty}^{\tau} rE_{\varphi} c d\tau \gg \frac{\partial}{\partial r} \int_{-\infty}^{\tau} rE_{\varphi} c d\tau,$$

and so on. We thus obtain

$$(2.9) \left\{ \begin{array}{l} rB_{\theta} = -rE_{\varphi} - \frac{1}{\sin \theta} \frac{\partial}{\partial \varphi} \int_{-\infty}^{\tau} E_r c d\tau, \\ rB_{\varphi} = rE_{\theta} + \frac{\partial}{\partial \theta} \int_{-\infty}^{\tau} E_r c d\tau, \\ \frac{\partial(rE_{\theta})}{\partial r} + 2\pi\sigma(rE_{\theta}) = -2\pi rJ_{\theta} + \frac{1}{2} \frac{\partial \bar{E}}{\partial \theta} \\ + \frac{1}{2 \sin \theta} \frac{\partial B_r}{\partial \varphi}, \\ \frac{\partial(rE_{\varphi})}{\partial r} + 2\pi\sigma(rE_{\varphi}) = -2\pi rJ_{\varphi} + \frac{1}{2 \sin \theta} \frac{\partial \bar{E}}{\partial \theta} \\ - \frac{1}{2} \frac{\partial B_r}{\partial r}, \end{array} \right.$$

where we have written

$$(2.10) \quad \bar{E} \stackrel{\text{def}}{=} E_r - \int_{-\infty}^{\tau} \frac{\partial E_r}{\partial r} c d\tau$$

for short. We do not drop the smaller integral in this case because it introduces no complication. On the other hand, it does extend the range in time over which the approximation is valid. All transverse field components can readily be obtained from Eqs. (2.9) and (2.10) once the longitudinal field components are known. For these components we have the equations

$$(2.11) \left\{ \begin{array}{l} \frac{1}{c} \frac{\partial E_r}{\partial \tau} + 4\pi\sigma E_r = -4\pi J_r + \frac{1}{r \sin^2 \theta} \\ \left\{ \frac{\partial}{\partial \theta} (\sin \theta B_{\varphi}) - \frac{\partial B_{\theta}}{\partial \varphi} \right\}, \\ \frac{1}{c} \frac{\partial B_r}{\partial \tau} = \frac{1}{r \sin \theta} \left\{ \frac{\partial E_{\theta}}{\partial \varphi} - \frac{\partial}{\partial \theta} (\sin \theta E_{\varphi}) \right\}. \end{array} \right.$$

How these equations are solved depends on whether we are concerned with a ground burst or an air burst. For the ground burst, the operator, $\partial/\partial\theta$, becomes very large near the ground and this allows an approximation scheme discussed in detail in Ref. 2.

In this report we confine our attention to a low-altitude air burst, in which case there are three possible asymmetries:

- a. Asymmetry of the bomb itself.
- b. Asymmetry resulting from vertical gradients of atmospheric properties such as density and water vapor content.
- c. The geomagnetic field.

All three of these are small effects, the second because atmospheric gradients are small, and the third because Compton electron range at low altitude is much shorter than its Larmor radius in the geomagnetic field. As the asymmetries are small, so also are the transverse components. Moreover the angular derivatives are small operators, of order $1/r$ or smaller. The result of this is that the transverse fields may be neglected in the radial E-equation giving

$$(2.12) \quad \frac{1}{c} \frac{\partial E_r}{\partial \tau} + 4\pi\sigma E_r = -4\pi J_r,$$

which is immediately integrable by quadratures. Formal integration of the radial B-equation yields

$$(2.13) \quad rB_r = \frac{1}{\sin \theta} \frac{\partial}{\partial \phi} \int_{-\infty}^{\tau} E_{\theta} c d\tau - \frac{1}{\sin \theta} \frac{\partial}{\partial \theta} \left[\sin \theta \int_{-\infty}^{\tau} E_{\phi} c d\tau \right].$$

Using this in the remaining equations, we see that the new terms involving integrals may be dropped for exactly the same reason as could the others and we have

$$(2.14) \quad \begin{cases} \frac{d(rE_{\theta})}{dr} + 2\pi\sigma(rE_{\theta}) = -2\pi rJ_{\theta} + \frac{1}{2} \frac{\partial \tilde{E}}{\partial \theta} \\ \frac{d(rE_{\phi})}{dr} + 2\pi\sigma(rE_{\phi}) = -2\pi rJ_{\phi} + \frac{1}{2 \sin \theta} \frac{\partial \tilde{E}}{\partial \phi} \end{cases}$$

Thus our procedure is first to solve Eq. (2.12) for E_r , next to calculate \tilde{E} from Eq. (2.10) and then Eqs. (2.14) are soluble by quadratures.

Note that the geomagnetic field enters solely through the quantities, J_{θ} and J_{ϕ} , whereas the other asymmetries enter solely through $\partial\tilde{E}/\partial\theta$ and $\partial\tilde{E}/\partial\phi$. Furthermore note that \tilde{E} will be a function of atmosphere density, ρ , of water vapor content, W , and of bomb asymmetry, γ . Thus we may write

$$(2.15) \quad \frac{\partial \tilde{E}}{\partial \theta} = \frac{\partial \rho}{\partial \theta} \frac{\partial \tilde{E}}{\partial \rho} + \frac{\partial W}{\partial \theta} \frac{\partial \tilde{E}}{\partial W} + \frac{\partial \gamma}{\partial \theta} \frac{\partial \tilde{E}}{\partial \gamma}.$$

In other words, the right-hand members of Eqs. (2.14) can be broken into a series of terms each of which expresses a single asymmetry. The same is therefore also true of the fields. We shall consider separately the individual asymmetries, knowing that the resulting signals may be combined linearly to obtain the total signal in the complex real situation.

III. THE SOURCE FUNCTIONS

The gamma rays from an explosion result from inelastic scattering of neutrons in the bomb materials themselves and in the air immediately surrounding the explosion. Other sources of gamma radiation such as neutron capture and fission fragment decay are of too low intensity to be of any importance to the prompt electromagnetic signal. During the reaction the neutron population in the bomb rises as $e^{\alpha\tau}$ and, after the peak which we conveniently define to be at $\tau = 0$, falls exponentially as $e^{-\delta\tau}$. Both α and δ are of order 10^8 /sec. The prompt gamma rays follow this same time history at the source. Fast neutrons which escape scatter in the air and, with every inelastic collision emit a gamma photon. It is easily seen that this population also decreases exponentially with time, say as $e^{-\kappa_2\tau}$, but as air density is much lower than that of bomb materials κ_2 is much less than δ , typically around 10^6 /sec. The air inelastic gamma rays also vary with time as $e^{-\kappa_2\tau}$. The Compton electron current is proportional to the gamma-ray flux and therefore varies as

$$(3.1) \quad J = -\mathcal{J}(r, \theta, \phi) f(\tau),$$

where

$$(3.2) \quad f(\tau) = \begin{cases} e^{\alpha\tau} & \text{for } \tau < 0, \\ e^{-\delta\tau} + \epsilon e^{-\kappa_2\tau} & \text{for } \tau > 0, \end{cases}$$

near the explosion.

The electromagnetic signal, however, comes mainly from a region which is 5 to 10 gamma-ray mean-free-paths, i.e. a distance of 1 to 2 kilometers, from the explosion. At such distances scattering strongly modifies the time history and the intensity of the gamma rays and the Compton current. A convenient way to describe these modifications is in terms of a build up factor, $B(r)$, which is the ratio of scattered to direct radiation at a distance, r , and of a response function, $u(r,\tau)$, which describes the time history of arrival of scattered gamma rays at a distance r from a δ -function source. Then at a distance r from the explosion, we have

$$(3.3) \quad J = -g(r, \delta, \varphi) \left\{ f(\tau) + B(r) \int_{-\infty}^{\tau} f(s)u(\tau-s)ds \right\},$$

where g includes the exponential absorption and $1/r^2$ attenuation of the unscattered beam.

A fair approximation to the response function, u , is the simple exponential, $\kappa_0 e^{-\kappa_0\tau}$, where κ_0 is constant in τ and varies slowly with r . In this case Eq. (2.3) readily works out to be

$$(3.4) \quad J = -g \begin{cases} \left[1 + \frac{\kappa_0 B}{\alpha + \kappa_0} \right] e^{\alpha\tau} & \text{for } \tau < 0 \\ e^{-\delta\tau} \left[1 - \frac{\kappa_0 B}{\delta - \kappa_0} \right] + \kappa_0 B e^{-\kappa_0\tau} \\ \left[\frac{1}{\alpha + \kappa_0} + \frac{1}{\delta - \kappa_0} - \frac{\epsilon}{\kappa_0 - \kappa_2} \right] \\ + \frac{\kappa_0 B \epsilon}{\kappa_0 - \kappa_2} e^{-\kappa_2\tau} & \text{for } \tau > 0. \end{cases}$$

Typically κ_0 is of order 10^7 so that it is considerably larger than κ_2 . At the large distances which interest us, the build up factor, B , is quite large, of the order 10, and therefore we see that J falls as $e^{-\kappa_0\tau}$ rather than $e^{-\delta\tau}$ throughout most of the prompt period.

At the large distances of interest to us, electron-ion recombination is completely negligible

and the conductivity, σ , can be separated into electronic conductivity, σ_e , and ionic conductivity, σ_i , governed by the equations

$$(3.5) \quad \begin{cases} \frac{d\sigma_e}{dt} + \beta\sigma_e = -A_e J \\ \frac{d\sigma_i}{d\tau} + a(\sigma_i)^2 = -A_i J \\ \sigma = \sigma_e + \sigma_i, \end{cases}$$

where β is the electron attachment rate in air, $\beta = 10^8$ /sec at S.T.P., and A_e is a factor depending on electron mobility, μ_e , the number, ν , of secondary electrons made by a primary, and the Compton electron path length in air, l , namely

$$(3.6) \quad A_e = \nu\mu_e/l.$$

The quantity, A_i , is the same thing but formed with twice the ion mobility, $2\mu_i$, instead of μ_e (two ion species), and a is the ion-ion recombination coefficient expressed in appropriate units. On our time scale it is quite accurate to set $a = 0$. Because the electron attachment time, β^{-1} , is so short, the conductivity, σ_e , follows the prompt source, $-A_e J$, except for a short period of duration about β^{-1} after the peak. Thus σ also rises as $e^{\alpha\tau}$ for $\tau < 0$ and falls as $e^{-\kappa_0\tau}$ at first. Later the conductivity levels off to a broad shoulder falling, let us say, as $e^{-\kappa_2\tau}$. This leveling off may occur because air inelastic gamma rays have caused J to level off. In the absence of air inelastic gamma rays, σ levels off because of the build up of ionic conductivity.

As we indicated above, $\kappa_0 e^{-\kappa_0\tau}$ is only a fair approximation to the scattering response function, $u(r,\tau)$. It can be made a good approximation, however, if we replace the constant, κ_0 , by a time dependent function, $\kappa(r,\tau)$. It follows, then, that except for a very short period of order, $(0 < \tau < 1/\beta)$, the conductivity can be accurately described by the expressions

$$(3.7) \quad \begin{cases} \sigma = \mathcal{L}_-(r, \delta, \varphi) e^{\alpha\tau} & \text{for } \tau < 0 \\ \sigma = \mathcal{L}_+(r, \delta, \varphi) \left\{ \kappa e^{-\int_0^{\tau} \kappa d\tau} + \eta e^{-\kappa_2\tau} \right\} & \text{for } \tau > 0. \end{cases}$$

with κ a slowly varying function of r and τ , η a slowly varying function of r , and κ_2 a constant. The $\tau > 0$ part of such a curve of σ vs. τ is shown in Fig. 1. The quantities, ζ_- and ζ_+ , are allowed to differ; in fact they must be so chosen that J is continuous at $\tau = 0$. From Eqs. (3.5) we now find

$$(3.8) \quad \begin{cases} J_r = -\frac{\beta + \alpha}{A_e} \dot{\zeta}_- e^{\alpha\tau} & \text{for } \tau < 0 \\ J_r = -\frac{\zeta_+}{A_e} \left\{ (\beta - \kappa + \dot{\kappa}/\kappa) \kappa e^{-\mu} \right. \\ \quad \left. + (\beta - \kappa_2) \tilde{\eta} e^{-\kappa_2\tau} \right\} & \text{for } \tau > 0. \end{cases}$$

Continuity at $\tau = 0$ yields

$$(3.9) \quad \zeta_- = \zeta_+ \left\{ \frac{\kappa_0(\beta - \kappa_0 + \dot{\kappa}_0/\kappa_0)}{\beta + \alpha} + \tilde{\eta} \frac{\beta - \kappa_2}{\beta + \alpha} \right\},$$

where dots mean $\partial/\partial\tau$ and zero subscripts mean the value at $\tau = 0$. We have defined

$$(3.10) \quad \mu \stackrel{\text{def}}{=} \int_0^\tau \kappa d\tau.$$

When there are many air inelastic gamma rays, the electronic conductivity levels off before ionic conductivity becomes important and we have

$$(3.11) \quad \eta = \tilde{\eta} \text{ (with air inelastic).}$$

In the absence of air inelastic gamma rays $\tilde{\eta}$ vanishes and

$$(3.12) \quad \begin{aligned} \sigma_i &= \frac{A_i}{A_e} \zeta_+ + \int_0^\tau (\beta - \kappa + \dot{\kappa}/\kappa) \kappa e^{-\mu} d\tau \\ &= \frac{A_i}{A_e} \zeta_+ \left[(\beta - \kappa_0) - (\beta - \kappa) e^{-\mu} \right]. \end{aligned}$$

Thus, as $(\beta - \kappa)A_i/\kappa A_e$ is very small

$$(3.13) \quad \eta = \frac{A_i}{A_e} (\beta_0 - \kappa_0), \quad \kappa_2 = 0 \text{ (no air inelastic)}$$

in the absence of air inelastic gamma rays. The peak

to shoulder ratio, κ_0/η , is normally of the order of 100 at distances of interest to us.

With the above general expressions for σ and for J we can calculate the radial E-field. For this we define two auxiliary quantities, S and E_s , defined by

$$(3.14) \quad S \stackrel{\text{def}}{=} \int_0^\tau 4\pi c \sigma d\tau$$

and

$$(3.15) \quad E_s \stackrel{\text{def}}{=} -J/\sigma.$$

From these definitions we readily see that

$$(3.16) \quad S = 4\pi c \zeta_+ \left[1 - e^{-\mu} + \frac{\eta}{\kappa_2} (1 - e^{-\kappa_2\tau}) \right]$$

for $\tau > 0$,

(S is undefined for $\tau < 0$), and

$$(3.17) \quad \begin{cases} E_s = E_\alpha = (\beta + \alpha)/A_e & \text{for } \tau < 0 \\ E_s = \frac{1}{A_e} \left\{ \frac{(\beta - \kappa + \dot{\kappa}/\kappa) e^{-\mu} + (\beta - \kappa_2)(\tilde{\eta}/\kappa) e^{-\kappa_2\tau}}{e^{-\mu} + (\eta/\kappa) e^{-\kappa_2\tau}} \right\} & \text{for } \tau > 0. \end{cases}$$

All of our equations so far are accurate except for a period of order $(1/\beta)$ after the peak. During this period, that portion of the signal which arises from asymmetry of E_r is very small and sizeable percentage errors here simply do not matter.

We can now solve Eq. (2.12) for E_r . In fact, from our definition above of E_s we see immediately that

$$(3.18) \quad E_r = e^{-\int_0^\tau 4\pi c \sigma d\tau'} \int_{-\infty}^\tau E_s e^{-\int_0^{\tau'} 4\pi c \sigma d\tau''} 4\pi c \sigma d\tau'.$$

As $E_s = E_\alpha = \text{constant}$ for $\tau < 0$ we have immediately

$$(3.19) \quad E_r(\tau) = E_\alpha \left[1 - e^{-4\pi c \sigma \tau} \right] \text{ for } \tau < 0.$$

For $\tau > 0$ we break the range of integration at $\tau = 0$ and we split S into two terms, writing

$$(3.20) \quad \begin{cases} s = S_0 - S_1 \\ S_0 = 4\pi c \dot{\omega}_+ , \\ S_1 = 4\pi c \dot{\omega}_+ \left\{ e^{-\mu} - \frac{\eta}{\kappa_2} (1 - e^{-\kappa_2 \tau}) \right\} \end{cases}$$

and obtain

$$(3.21) \quad E_r(\tau) = E_r(-0)e^{-S(\tau)} + e^{S_1(\tau)} \int_0^\tau E_s(\tau') e^{-S_1(\tau')} 4\pi c d\tau' ,$$

where $E_r(-0)$ is given by evaluating Eq. (3.19) at $\tau = 0$.

Note that S_1 becomes much smaller than S_0 after a period of a few times $(\kappa_0)^{-1}$. During this short period when the two are comparable, E_s varies but little and this circumstance enables us to evaluate the integral of Eq. (3.21) to good precision, obtaining simply

$$(3.22) \quad E_r(\tau) = E_r(-0)e^{-S} + E_0[1 - e^{-S}] ,$$

where E_0 is the value of E_s obtained by evaluating Eq. (3.17) at $\tau = +0$. The details of evaluating the integral to obtain Eq. (3.22) are all worked out in Appendix A. Even Eq. (3.22) can be simplified. As we shall see, at times in the neighborhood of the peak the signal comes from a very narrow region about the point $r = R_s$ where $2\pi\sigma = 1/\lambda$, very nearly. In this neighborhood, therefore, $4\pi c\sigma/\alpha$ is very small and

$$(3.23) \quad E_r(-0) \approx E_0 \cdot \frac{2c}{\alpha\lambda} \ll E_0$$

so that the term in $E_r(-0)$ may be dropped, giving

$$(3.24) \quad E_r = E_0(1 - e^{-S}) .$$

As we shall see, carrying the term in $E_r(-0)$ would introduce no additional complication, but would not contribute noticeably to the signal.

In order to evaluate the integrals required to calculate the radiated fields, it is convenient here to define a new function, k , by the relation

$$(3.25) \quad k \stackrel{\text{def}}{=} S/\sigma = 4\pi c \left\{ \frac{1 - e^{-\mu} + (\eta/\kappa_2)(1 - e^{-\kappa_2 \tau})}{\kappa e^{-\mu} + \eta e^{-\kappa_2 \tau}} \right\} ,$$

for $\tau > 0$.

so that Eq. (3.24) may be written as

$$(3.26) \quad E_r(\tau) = E_0(1 - e^{-k\sigma}) \text{ for } \tau > 0 .$$

We see that k depends only weakly on position but strongly on τ .

To complete our evaluation of the source function we need the time integral of Eq. (3.26). From Eq. (3.16) we see that S , i.e. $k\sigma$, is essentially constant in τ except for the first couple of generations after the peak. Therefore we can write

$$(3.27) \quad \int_0^\tau E_r c d\tau = E_0(1 - e^{-k\sigma})c\tau$$

to good precision, for when τ is so small that $k\sigma$ is varying this expression does not differ significantly from zero. Thus we have

$$(3.28) \quad \bar{E} \stackrel{\text{def}}{=} E_r - \int_0^\tau \frac{\partial E_r}{\partial r} c d\tau = \left(E_0 - c\tau \frac{\partial E_0}{\partial r} \right) (1 - e^{-k\sigma}) + E_0 Z c \tau k \sigma e^{-k\sigma} ,$$

where Z is defined by

$$(3.29) \quad Z \stackrel{\text{def}}{=} \frac{1}{k\sigma} \frac{\partial(k\sigma)}{\partial r} .$$

Clearly Z is about $1/\lambda$ and the correction term to E_r would not be needed for $c\tau \ll \lambda$. We keep the correction term in order not to be restricted by such a severe limitation. The source function for atmospheric and for bomb asymmetries is obtained by differentiating Eq. (3.28), and is

$$(3.30) \quad \frac{\partial \bar{E}}{\partial \theta} = \left[\frac{\partial E_0}{\partial \theta} - c\tau \frac{\partial^2 E_0}{\partial \theta \partial r} \right] [1 - e^{-k\sigma}] + \left[\Omega E_0 - c\tau \left(\Omega \frac{\partial E_0}{\partial r} - Z \frac{\partial E_0}{\partial \theta} - E_0 \frac{\partial Z}{\partial \theta} \right) \right] k \sigma e^{-k\sigma} + \Omega E_0 Z c \tau [k\sigma - (k\sigma)^2] e^{-k\sigma} .$$

where we have written for short

$$(3.31) \quad \Omega \stackrel{\text{def}}{=} \frac{1}{k\sigma} \frac{\partial(k\sigma)}{\partial\theta} .$$

The terms proportional to τ , which arise from Eq. (3.27), we shall call the secular terms; they are clearly of importance only when $c\tau/\lambda$ is appreciable.

In deriving Eq. (3.30) we have allowed specifically for all effects of gamma-ray scattering except for one, namely the change of angular distribution of Compton electrons with distance and with time. This effect can, however, be included by simply redefining the quantity, ν , the effective number of secondary electrons per Compton electron, to be a function of τ and of r . This introduces additional τ and r dependence of E_s , but we already have specifically allowed E_s to depend on these quantities. Thus, with proper interpretation, our results are quite general.

IV. SPECIFIC SOLUTIONS

We have seen that the geomagnetic signal can be discussed separately from the other signals. As this signal has been discussed quite well elsewhere and is well understood,^(3,4,5) we content ourselves here with deriving the basic formula which we do simply for completeness. We consider a perfectly symmetrical explosion in a perfectly uniform atmosphere but in the presence of a uniform magnetic field, B_0 . Choosing our polar axis in the direction of $-B_0$ we find

$$(4.1) \quad J_\varphi = \frac{l}{2a} J \sin \vartheta, \quad J_\theta = 0,$$

where l is Compton electron range, a is its gyro radius in the geomagnetic field and J is the radial Compton current. Our only surviving field equation is

$$(4.2) \quad \frac{\partial(rE_\varphi)}{\partial r} + 2\pi\sigma(rE_\varphi) = -2\pi rJ \left(\frac{l}{2a}\right) \sin \vartheta,$$

whose solution is

$$(4.3) \quad rE_\varphi = \frac{l \sin \vartheta}{2a} e^X \int_0^r rE_s e^{-X} 2\pi\sigma dr,$$

where

$$(4.4) \quad X \stackrel{\text{def}}{=} \int_r^\infty 2\pi\sigma dr.$$

At large distances we can set $r = \infty$ in the right-hand side and obtain for the radiated signal

$$(4.5) \quad rE_\varphi = \frac{l \sin \vartheta}{2a} \int_0^\infty rE_s e^{-X} 2\pi\sigma dr.$$

The factor, $2\pi\sigma e^{-X}$, has a very sharp maximum at $r = \bar{R}_s$, the point at which

$$(4.6) \quad 2\pi\sigma = Z = -\frac{1}{\sigma} \frac{\partial\sigma}{\partial r}.$$

This fact enables us to evaluate the integral. The details are given in Appendix B and, to lowest order in λ/\bar{R}_s , we obtain the well-known formula

$$(4.7) \quad rE_\varphi = \frac{l \sin \vartheta}{2a} \cdot \bar{R}_s E_s(\bar{R}_s, \tau).$$

So long as \bar{R}_s is considerably larger than λ , Eq.(4.6) above indicates that it is proportional to $\log \sigma$. E_s is constant during the α -phase and changes rapidly at the peak, dropping to a lower nearly constant value during the κ -phase. Thus the geomagnetic signal is a short, sharp spike having its peak slightly before σ reaches maximum.

We now address ourselves in somewhat more detail to the other asymmetries. We may ignore geomagnetic effects, setting $J_\varphi = J_\theta = 0$. It is convenient to choose our polar axis vertical. If then we suppose that the bomb itself is azimuthally symmetric, so will be the field equations, which reduce to

$$(4.8) \quad \frac{\partial(rE_\theta)}{\partial r} + 2\pi\sigma(rE_\theta) = \frac{1}{2} \frac{\partial E}{\partial \theta},$$

which has the solution

$$(4.9) \quad rE_\theta = e^X \int_0^r \frac{1}{2} \frac{\partial \tilde{E}}{\partial \theta} e^{-X} dr,$$

X being the quantity defined above in Eq. (4.4). We confine our attention to the distant field, writing

$$(4.10) \quad rE_{\theta} = \int_0^{\infty} \frac{1}{2} \frac{\partial \tilde{E}}{\partial \theta} e^{-X} dr,$$

and shall refer to this as the radiated signal. If we now substitute for $\partial \tilde{E} / \partial \theta$ the expression given by Eq. (3.30) we obtain

$$(4.11) \quad rE_{\theta} = \int_0^{\infty} \varphi_1 [1 - e^{-k\sigma}] e^{-X} dr \\ + \int_0^{\infty} \varphi_2 k \sigma e^{-k\sigma - X} dr + \int_0^{\infty} \varphi_3 [k\sigma - (k\sigma)^2] e^{-k\sigma - X} dr,$$

where $\varphi_1, \varphi_2, \varphi_3$ are given by

$$(4.12) \quad \begin{cases} \varphi_1 = \frac{1}{2} \left[\frac{\partial E_0}{\partial \theta} - c\tau \frac{\partial^2 E_0}{\partial r \partial \theta} \right], \\ \varphi_2 = \frac{1}{2} \left[\Omega E_0 + c\tau \left(E_0 \frac{\partial Z}{\partial \theta} + Z \frac{\partial E_0}{\partial \theta} - \Omega \frac{\partial E_0}{\partial r} \right) \right], \\ \varphi_3 = \frac{1}{2} \Omega E_0 Z c\tau. \end{cases}$$

We have defined Z and Ω in Eqs. (3.29) and (3.31).

Now consider for a moment the second term of Eq. (4.11). The factor, $k\sigma \exp[-k\sigma - X]$, is a rapidly varying function of r with a sharp maximum at $r = R_s$, that value of r for which

$$(4.12a) \quad 2\pi\sigma y = Z, \quad y \stackrel{\text{def}}{=} 1 + kZ/2\pi.$$

On the other hand φ_2 is a slowly varying function of r and this enables one to evaluate the integral without specifying the functional forms of φ and of σ . In Appendix B this is worked out in detail, as are also the first and third integrals. In this Appendix expansions are given out to third order in (λ/R_s) . As this quantity is normally about 1/10, it normally suffices to take the first terms of these expansions obtaining the result

$$(4.13) \quad rE_{\theta} = \left[\frac{\varphi_1}{Z} \log y + \frac{\varphi_2 k}{2\pi y} + \frac{\varphi_3 k}{2\pi y^2} \right]_{r=R_s}.$$

If higher order accuracy is required, additional correction terms will be found in Appendix B, along with error estimates.

The quantity, k , [Eq. (3.2)] is a rapidly varying function of τ and, at most, a slowly varying function of r . The φ 's, on the other hand, vary at most linearly with τ . Normally φ_3 is of the same order as the secular term of φ_2 and, as y becomes quite large, the term in φ_3 is a relatively small correction.

We can now dispose of the α -phase in a general way. During this period we have $k = 4\pi c/\alpha$ and Z is very nearly $1/\lambda$ so that

$$(4.14) \quad rE_{\theta} = \lambda \varphi_1 \log \left(1 + \frac{2c}{\alpha \lambda} \right) + \varphi_2 \frac{2c/\alpha}{1 + 2c/\alpha \lambda} \\ + \varphi_3 \frac{2c/\alpha}{(1 + 2c/\alpha \lambda)^2}.$$

But $2c/\alpha \lambda \ll 1$ and the terms of $\varphi_1, \varphi_2, \varphi_3$ which are proportional to τ are completely negligible at this stage. Thus we may expand Eq. (4.14) and obtain

$$(4.15) \quad rE_{\theta} = \frac{c}{\alpha} E_{\alpha} \left\{ \frac{1}{E_{\alpha}} \frac{\partial E_{\alpha}}{\partial \theta} + \frac{1}{\sigma} \frac{\partial \sigma}{\partial \theta} \right\} \text{ for } \tau < 0,$$

where E_{α} is the (constant) value of E_s when $\tau < 0$. The signals which come later are clearly of order λE_0 which is much larger than $2cE_{\alpha}/\alpha$. We can therefore completely ignore the α -stage signal.

For $\tau > 0$ the radiated signal behaves essentially like the first two terms of Eq. (4.13), the third remaining always a small correction. Thus, aside from the secular terms, which are important only when τ approaches a microsecond or so, the signal is given by a linear combination of the two functions of τ , $\log y$ and $Zk/2\pi y$. Over most of the range of τ , $Zk/2\pi$ is large and these become slowly varying functions of k and hence insensitive to its details. This becomes clearest if we examine these quantities not as functions of real time, τ , but rather as functions of generation number, Γ , which we define as

$$(4.16) \quad \Gamma \stackrel{\text{def}}{=} \int_{jL}^{\tau} \text{sign } \tau \left[\log (\sigma_{\text{peak}}/\sigma(\tau)) \right]_{r=R_s}.$$

In Fig. 2 we have plotted the two functions

$$(4.17) \begin{cases} F(\Gamma) = \log(1 + k/2\pi\lambda) \\ G(\Gamma) = \frac{k/2\pi\lambda}{1 + k/2\pi\lambda} \end{cases}$$

as functions of the generation number, Γ . Each was calculated for two different cases, namely:

- a. The solid curves are computed from the σ vs. τ history of Fig. 1. This case is described by a prompt burst with κ varying from an initial value of 2.8×10^7 to a final value of 3.8×10^6 , plus a long tail of air inelastic gammas for which $\kappa_2 = 4 \times 10^5$. The peak to shoulder ratio, (κ_0/η) , is 70.
- b. The dotted curves are computed for a prompt burst of constant κ , $\kappa = \kappa_0 = 2.24 \times 10^7$ and without any long tail to σ .

The curves of case a. correspond to a σ history which is far from being a simple exponential, yet the dotted and the solid curves lie remarkably close to one another. It is clear that for many purposes "universal" curves for the two functions, F and G , would suffice. In addition, of course, one would need a σ vs. τ curve to translate generation number, Γ , into real time and for times not much less than λ/c the secular terms in φ_1 and φ_2 would have to be included.

We shall now proceed to discuss in detail special cases. We have in every case retained all the secular terms, including the small one in φ_3 but have calculated only to lowest order in (λ/R_s) , which we have supposed to be 1/10. In all cases calculations were made for the two σ vs. τ histories designated as a. and b. above. Curves are shown (case a-solid, case b-dotted) for normalized signal strength vs. generation number Γ and also vs. real time, τ . For the quantity, Z , itself, we have used simply $1/\lambda$, but have used higher order terms to compute $\partial Z/\partial \theta$.

A. Bomb Asymmetry Alone

If the only asymmetry is that of the bomb itself, then J and σ have identical angular dependences,

which may be written as

$$(4.18) \begin{cases} J = J(r, \tau) \cdot \omega(\theta) \\ \sigma = \sigma(r, \tau) \cdot \omega(\theta) \\ \Omega = \partial\omega/\partial\theta \end{cases}$$

Thus E_θ is independent of θ ; as there is no atmospheric gradient it is also independent of r and Eq. (4.13) reduces to

$$(4.19) \quad rE_\theta = \frac{1}{2} \lambda E_0 \Omega \frac{k/2\pi\lambda}{1 + k/2\pi\lambda} \left\{ 1 + \frac{c\tau/\lambda}{1 + k/2\pi\lambda} \right\}.$$

In case b. the secular term is completely unimportant, in case a. it never exceeds 0.1, and this only after 1 microsecond. Thus this signal is essentially described by the function, G . Curves are shown in Figs. 3 and 4 giving rE_θ vs. generation number, Γ , and real time, τ , respectively.

B. Gradient in Water Vapor Concentration

Next consider a perfectly symmetric explosion in an atmosphere of uniform density. However, owing to a gradient in water vapor concentration, the electron mobility, and hence σ , varies with altitude. If, for convenience, we take the variation to be of the form

$$(4.20) \quad \mu_e = \mu_0 \exp\left\{-\frac{r}{h} \cos \theta\right\}$$

we find

$$(4.21) \quad \begin{cases} \varphi_1(R_s) = -\frac{R_s \sin \theta}{2h} E_0 \left[1 - \frac{c\tau}{R_s} \left(1 + \frac{R_s \cos \theta}{h} \right) \right] \\ \varphi_2(R_s) = \frac{R_s \sin \theta}{2h} E_0 \left[1 - \frac{c\tau}{\lambda} \left(1 + \frac{2\lambda}{R_s} + \frac{2\lambda \cos \theta}{h} \right) \right] \\ \varphi_3(R_s) = \frac{R_s \sin \theta}{2h} E_0 \cdot \frac{c\tau}{\lambda} \left[1 + \frac{\lambda}{R_s} + \frac{\lambda \cos \theta}{h} \right] \end{cases}$$

Assuming one is near enough to the equatorial plane that $R_s \cos \theta/h \ll 1$, the radiated signal is

$$(4.22) \quad rE_\theta = \lambda E_0 \left(\frac{R_s \sin \theta}{2h} \right)$$

$$\left\{ \left[1 - \frac{c\tau}{\lambda} \frac{k/2\pi\lambda}{1 + k/2\pi\lambda} \right] \frac{k/2\pi\lambda}{1 + k/2\pi\lambda} - \left(1 - \frac{c\tau}{R_s} \right) \log(1 + k/2\pi\lambda) \right\},$$

to lowest order in λ/R_s . Here the secular term is of order $c\tau/\lambda$ and quite important at 1 microsecond. Curves of rE_θ vs. generation number, Γ , and real time, τ , are shown in Figs. 5 and 6, respectively.

C. Atmospheric Density Gradient

At low altitudes air density varies exponentially with the altitude so that we may write

$$(4.23) \quad \rho = \rho_0 \exp \left\{ -r \cos \theta / H \right\}.$$

The quantity, H , is called the relaxation height and may be taken to be about 9 kilometers. In this subsection we shall always use the subscript 0 to indicate the value of a quantity at burst altitude. As electron attachment is a three-body process, the attachment coefficient, β , varies as ρ^2 so that

$$(4.24) \quad \beta = \beta_0 e^{-2r \cos \theta / H}.$$

Now writing

$$(4.25) \quad J = -\mathcal{J}(r, \theta) \cdot F(\tau),$$

we can write for \mathcal{J} ,

$$(4.26) \quad \mathcal{J} = \frac{bY}{\lambda_0} \left[\frac{1}{r} - \frac{\cos \theta}{2H} \right] \exp \left[-\frac{r}{\lambda_0} \left(1 - \frac{r \cos \theta}{2H} \right) \right]$$

so long as we confine ourselves to regions sufficiently near the equatorial plane that $R_s \cos \theta / H \ll 1$. The bomb yield expressed in appropriate units is Y and b is a constant arising from an empirical fit to the build-up factor. The details are given in Appendix C.

In calculating derivatives of E_s from Eq. (3.15) we shall ignore any dependence of κ , η , and A_e on position as we do not at present know these. Thus we write

$$(4.27) \quad \frac{\partial E_s}{\partial \theta} = \frac{1}{A_e} \frac{\partial \beta}{\partial \theta} = \frac{\beta_0}{A_e} \cdot \frac{2r \sin \theta}{H},$$

$$\frac{\partial E_s}{\partial r} = -\frac{\beta_0}{A_e} \frac{2 \cos \theta}{H}.$$

With Eqs. (4.26) and (4.27) and the relation, $\sigma = J/E_s$, we can calculate the functions φ_1 , φ_2 , and φ_3 . When the result of this calculation is set into Eq. (4.13) we obtain

$$(4.28) \quad rE_\theta = \frac{\lambda_0 R_s E_0}{4H} \sin \theta$$

$$\left\{ \frac{4\beta_0}{A_e E_s} \left(1 - \frac{c\tau}{R_s} \right) \left(1 - \frac{\lambda_0}{R_s} \right) \log \left(1 + \frac{k}{2\pi\lambda_0} \right) - \frac{R_s}{\lambda_0} \left(\frac{k/2\pi\lambda_0}{1 + k/2\pi\lambda_0} \right) \left[1 + \frac{\lambda_0}{R_s} \left(\frac{4\beta_0}{A_e E_s} - 1 \right) + \frac{c\tau/\lambda_0}{1 + k/2\pi\lambda_0} - \frac{c\tau}{R_s} \left(2 + \frac{4\beta_0}{A_e E_s} \left[\frac{k/2\pi\lambda_0}{1 + k/2\pi\lambda_0} \right] + \frac{\lambda_0}{R_s} \left[\frac{8\beta_0}{A_e E_s} - 1 \right] \right) \right] \right\},$$

correct through first order in λ/R_s . As $\beta_0/A_e E_s \approx 1$ and $\lambda/R_s \approx 1/10$ we see that the secular terms are again of order $c\tau/\lambda$. Curves of this signal vs. generation number, Γ , and real time, τ , are shown in Figs. 7 and 8, respectively.

V. DISCUSSION AND CONCLUSIONS

We have shown how the early portion of the radio flash from a low-altitude air burst may be computed. Use of the high-frequency approximation enables us to obtain simple analytic expressions for the signal starting from a quite general σ vs. τ history. A question still unanswered remains, namely, for how long a time is the approximation valid? To answer this question we have used the solutions found to estimate those terms of Maxwell's equations which were originally dropped. Inserting these estimates into Maxwell's equations, one can solve and obtain first-order corrections to the high-frequency approximation. This process is carried out in detail in Appendix D, where it is shown that the fractional error involved in using the high-frequency approximations is about $c\tau/R_s$, R_s being our usual signal radius defined by Eq. (4.12a), that is to say, the approximation is good so long as

$$(5.1) \quad c\tau \ll R_s.$$

Typically this means that we can have confidence in about the first microsecond of the computed waveform. It should be pointed out here that condition (5.1) was achieved by including the secular terms, which our earlier theory did not do. Without these secular terms the much more stringent condition

$\sigma \ll \lambda$ must be fulfilled.

The second conclusion we wish to point out is the limited variety of possible pulse shapes. Leaving aside the geomagnetic signal, we saw that all other asymmetries lead roughly to signals which are linear combinations of two basic pulse shapes, described by the functions, F and G, of Eq. (4.17). Because of the presence of the secular terms, this is not strictly true; nevertheless, it is true in a practical sense as illustrated in Fig. 9. In this figure we have plotted as a solid line the atmospheric asymmetry signal of Fig. 8 (solid line), together with the dotted curve which is a linear combination of the bomb asymmetry signal and water vapor gradient signal (solid lines) of Figs. 4 and 5. The linear combination chosen is an improbable one, but it does show that there are essentially only two independent pulse shapes. This should, of course, have been obvious from the beginning, for there are only two basic asymmetries, that of J and that of σ . Practically, this means that inclusion of new effects, such as the spatial dependence of A_e and of κ , will introduce no new pulse shapes. It also means that it is impossible to sort out the various asymmetries from a given signal.

There is one effect which we have not included in our calculations which might lead to an additional wiggle in the curve, and that is the effect of differential scattering. Owing to the density gradient of the atmosphere more of the gamma rays arriving at some distant point r have been scattered downward than upward. This will produce a net current of Compton electrons downward at the point in question, i.e., a negative J_θ . The signal produced by this J_θ is calculated exactly as was the geomagnetic signal and will in fact resemble the latter signal, with two important differences:

- a. Because only scattered gammas contribute, the signal will be delayed and broadened as compared with the geomagnetic signal.
- b. The polarity of the signal will be positive regardless of magnetic bearing.

A rough estimate indicates that the amplitude of this signal is small, but further consideration of it is surely warranted. ⁽⁸⁾

Nonlinear effects have been omitted from our theory; in fact they are negligibly small. As the signal comes from a thin shell centered on $r = R_s$, it suffices to confine our attention to this region. Using the formulas we have developed for E_r at this position we see that this quantity is simply not large enough to extract a significant fraction of the Compton electron energy. The transverse fields are ineffective in producing a transverse J for the simple reason that E_θ, H_ϕ are very nearly a pure radiation field so that their effects on the Compton electrons very nearly cancel. The only nonlinear effect remaining is the field dependence of the electron mobility, μ_e , and the attachment coefficient, β . Over a wide range of field strength, β and μ_e depend on the electric field as ⁽⁶⁾

$$(5.2) \quad \mu_e = \mu_0 \sqrt{E}, \quad \beta = \beta_0 \sqrt{E},$$

where numerically $\mu_0 = 10^6$ and $\beta_0 = 10^8$ when E is expressed in e.s.u. During the κ -phase, the electric conductivity depends on these parameters as

$$(5.3) \quad \sigma \propto \frac{\mu_e}{\beta - \kappa} = \frac{\mu_0}{\beta_0 - \kappa \sqrt{E}}.$$

It turns out that κ is so much smaller than β that the nonlinearity of μ_e is essentially cancelled by that of β and the field dependence of σ is so weak that it can be safely ignored. During the α -phase we do not necessarily have $\alpha \ll \beta$. On the other hand the radial E-field at $r = R_s$ is very small during this phase, around 0.03 e.s.u. or less. At such low field strength the conduction electrons are essentially thermal and μ_e, β are no longer field dependent.

APPENDIX A - THE RADIAL E-FIELD

According to Eq. (3.21) the problem of calculating the radial E-field is solved once we evaluate the integral

$$(A.1) \quad I \stackrel{\text{def}}{=} \int_0^r E_s e^{-S_1} l_{4\pi c \sigma dr'},$$

$$(B.15) \quad \bar{I} = \int_r^\infty \varphi e^{-\psi} 2\pi \alpha dr = - \int_r^\infty \left(\frac{\varphi}{y} \right) (e^{-\psi} \psi' dr) ,$$

which partially integrates to yield

$$(B.16) \quad \bar{I} = \frac{\varphi}{y} (1 - e^{-\psi}) + \int_r^\infty \left(\frac{\varphi}{y} \right)' (1 - e^{-\psi}) dr .$$

Using Eq. (B.11), this may be written as

$$(B.17) \quad \bar{I} = \frac{\varphi}{y} (1 - e^{-\psi}) - \int_r^\infty \frac{1 + w(\frac{\varphi}{y})'}{z} \left[\frac{1 - e^{-\psi}}{\psi} \psi' dr \right] ,$$

and we can integrate by parts again obtaining

$$(B.18) \quad \bar{I} = \frac{\varphi}{y} (1 - e^{-\psi}) + \frac{1 + w(\frac{\varphi}{y})'}{z} [\gamma + \log \psi + E_1(\psi)] + \int_r^\infty \left[\frac{1 + w(\frac{\varphi}{y})'}{z} \right]' [\gamma + \log \psi + E_1(\psi)] dr ,$$

where γ is the Euler-Mascheroni constant, $\gamma = 0.5772156 \dots$.

Now put $r = R_s$ into Eqs. (B.13) and (B.18) and add. We obtain

$$(B.19) \quad \int_0^\infty \varphi e^{-\psi} 2\pi \alpha dr = \left[\frac{\varphi}{y} \left\{ 1 + \frac{1 + w(\frac{\varphi}{y})'}{z} \left(\frac{\varphi}{\varphi} - \frac{y'}{y} \right) (\gamma + \log \psi) \right\} \right]_{r=R_s} + \dots .$$

The remainder, indicated above by the dots, is readily estimated with the aid of the integrals of Eqn. (B.13) and (B.18). The outer region contributes

$$(B.20) \quad \epsilon_{\text{ext}} = \int_{R_s}^\infty \left[\frac{1 + w(\frac{\varphi}{y})'}{z} \right]' \sum_{n=1}^\infty \frac{(-)^{n-1} \psi^{n-1}}{n n!} dr$$

$$\approx \left[\frac{1 + w(\frac{1 + w(\frac{\varphi}{y})'}{z})'}{z} \right]_{r=R_s} \int_0^\psi \sum_{n=1}^\infty \frac{(-)^{n-1} \psi^{n-1}}{n n!} d\psi$$

$$= \left[\frac{1 + w(\frac{1 + w(\frac{\varphi}{y})'}{z})'}{z} \right]_{r=R_s} \cdot \sum_{n=1}^\infty \frac{(-)^{n-1} \psi_s^{n-1}}{n^2 n!} .$$

Similarly the inner region contributes

$$(B.21) \quad \epsilon_{\text{int}} = \int_0^{R_s} \frac{1 + w(\frac{1 + w(\frac{\varphi}{y})'}{z})'}{z} \frac{E_1(\psi)}{\psi} \psi' dr$$

$$\approx \left[\frac{1 + w(\frac{1 + w(\frac{\varphi}{y})'}{z})'}{z} \right]_{r=R_s} \int_{\psi_s}^\infty \frac{E_1(\psi)}{\psi} d\psi .$$

Chandrasekhar⁽⁷⁾ gives as the value of this integral

$$(B.22) \quad \int_{\psi_s}^\infty \frac{E_1(\psi)}{\psi} d\psi = \frac{1}{2} \gamma^2 + \frac{\pi^2}{12} - \sum_{n=1}^\infty \frac{(-)^{n-1} \psi_s^{n-1}}{n^2 n!}$$

whence we find

$$(B.23) \quad \epsilon_{\text{Tot}} \approx \left[\frac{\gamma^2}{2} + \frac{\pi^2}{12} \right] \left[\frac{1 + w(\frac{1 + w(\frac{\varphi}{y})'}{z})'}{z} \right]_{r=R_s}$$

very nearly. The error is worst at late times such that $kz/2\pi$ is large. Setting $z \approx 1/\lambda$ the fractional error is about

$$(B.24) \quad \epsilon_{\text{Tot}}/I_1(\infty) \approx \lambda^2 \left\{ -\frac{2\lambda}{R_s^2} + \frac{\psi \lambda (\frac{\varphi}{y})'}{R_s^2 (\frac{\varphi}{y})} + \left(\frac{\varphi''}{\varphi} \right)_s \right\} .$$

For functions, φ , which vary as some low power of r this error is about 10% if R_s is as small as 5λ .

For yields of reasonable magnitude R_s is more like 10λ and the error becomes quite small. If to Eq. (B.19) we add the correction term, Eq. (B.23), the remaining error is of order $(\lambda/R_s)^3$ and thus small even for such tiny yields as $R_s = 3\lambda$.

Applying Eq. (B.5) to Eq. (B.19) yields

$$(B.24) \quad \int_0^{\infty} \varphi(1 - e^{-k\sigma})e^{-X}dr$$

$$= \left[\frac{\varphi}{z} \left\{ \log y + \frac{1+w}{z} (\gamma + \log \psi) \right\} \left[\left(\frac{\varphi'}{\varphi} - \frac{z'}{z} \right) \log y + \frac{kz'}{2\pi y} \right] \right]_{R_s}$$

Similarly, from Eq. (B.4) we have

$$(B.25) \quad \int_0^{\infty} \varphi 2\pi(\sigma)^2 e^{-\psi} dr = \left[\frac{z\varphi}{2\pi y^2} \right]_{r=R_s} + \dots$$

In order to calculate second-order corrections to the field quantities we also need I_1 and I_2 as functions of a running upper limit; I_3 however is needed only in correction terms, which is why it is given above to first order only. We have already calculated $I_1(r)$ and we can see that, as $\varphi(r)$ is presumed to vary slowly with r , we have to first order

$$(B.26) \quad \int_0^r \varphi e^{-\psi} 2\pi\sigma dr = \begin{cases} \frac{\varphi(r)}{y(r)} e^{-\psi(r)} & \text{for } r \leq R_s \\ \frac{\varphi_s}{y_s} e^{-\psi(r)} & \text{for } r \geq R_s, \end{cases}$$

where subscript s means evaluation at $r = R_s$. Now from Eq. (B.5) it follows that

$$(B.27) \quad \int_0^r \varphi(1 - e^{-k\sigma})e^{-X}dr = \begin{cases} \frac{\varphi}{z} \left[E_1\left(\frac{2\pi\sigma}{z}\right) - E_1\left(\frac{2\pi\sigma y}{z}\right) \right] e^{\frac{2\pi\sigma}{z} - X} & \text{for } r \leq R_s \\ \frac{\varphi_s}{z_s} \left[E_1\left(\frac{2\pi\sigma}{z_s}\right) - E_1\left(\frac{2\pi\sigma y_s}{z_s}\right) \right] e^{\frac{2\pi\sigma}{z_s} - X} & \text{for } r \geq R_s. \end{cases}$$

As these quantities are used only in correction terms, we do not need higher order accuracy.

APPENDIX C - CURRENT DENSITY IN A NONUNIFORM ATMOSPHERE

If we write out Eq. (3.3) specifically for a uniform atmosphere we should have

$$(C.1) \quad J = -\frac{Y e^{-r/\lambda}}{r^2} \{f(\tau) + B(r)F(\tau)\},$$

where we have written $F(\tau)$ for the falting integral of Eq. (3.3) and Y represents the yield in appropriate units; λ is of course the gamma ray mean-free-path. The build-up factor is quite well represented empirically by

$$(C.2) \quad B(r) = b \left(\frac{r}{\lambda} \right),$$

with b a constant. For distances such as $r \approx 10\lambda$, it turns out that $B \gg 1$ and we can in fact write

$$(C.3) \quad J = -g(r) \cdot F(\tau),$$

where

$$(C.4) \quad g = \frac{bY e^{-r/\lambda}}{r^2} \left(\frac{r}{\lambda} \right).$$

Sometimes in fitting $B(r)$, an exponential factor is included on the right-hand side of Eq. (C.2), but this merely leads to a redefinition of λ in our Eq. (C.4).

In an exponential atmosphere, λ is no longer a constant but is given by

$$(C.5) \quad \frac{1}{\lambda} = \frac{1}{\lambda_0} e^{-r \cos \theta/H},$$

In Eq. (C.4) r/λ means the distance measured in mean-free-paths and therefore, in case of a variable density we must make the replacement

$$(C.6) \quad \frac{r}{\lambda} \rightarrow \int_0^r \frac{dr}{\lambda} = \frac{H}{\lambda_0 \cos \vartheta} [1 - e^{-r \cos \vartheta / H}] .$$

When this replacement is made, Eq. (C.4) is found to correspond with

$$(C.7) \quad \eta = \frac{YbH}{r^2 \lambda_0 \cos \vartheta} [1 - e^{-r \cos \vartheta / H}] \exp \left[-\frac{H}{\lambda_0 \cos \vartheta} (1 - e^{-r \cos \vartheta / H}) \right]$$

in the case of the atmosphere of variable density.

In the end this quantity and its derivatives will be evaluated at $r = R_s$. At low altitudes R_s is considerably less than H . Moreover the signal is frequently observed near the equatorial plane so that

$$(C.8) \quad R_s \cos \theta \ll H .$$

When this is true we can expand some of the exponentials simplifying η to

$$(C.9) \quad \eta = \frac{bY}{\lambda_0} \left[\frac{1}{r} - \frac{\cos \theta}{2H} \right] \exp \left[-\frac{r}{\lambda_0} \left(1 - \frac{r \cos \vartheta}{2H} \right) \right] ,$$

which is Eq. (4.26) of the main text.

APPENDIX D - LIMIT OF VALIDITY OF THE HIGH-FREQUENCY APPROXIMATION

In making the high-frequency approximation, certain terms were dropped from Maxwell's equations because they are unimportant at early times. Now that we have obtained such a zero-order approximation to the fields, we can use these results to calculate the values of the terms dropped from Maxwell's equations. These additional source terms enable us to calculate first-order corrections to the fields, and in principle one could continue, writing

$$(D.1) \quad \begin{cases} E_r = E_r^{(0)} + E_r^{(1)} + \dots , \\ E_\theta = E_\theta^{(0)} + E_\theta^{(1)} + \dots , \\ B_\varphi = B_\varphi^{(0)} + B_\varphi^{(1)} + \dots . \end{cases}$$

We shall carry out this program as far as the correction $E_\theta^{(1)}$ to the radiated field. Our aim in this calculation is not to achieve higher order accuracy of the fields but rather to define the time interval for which the zero-order solution is valid. Thus we shall content ourselves with somewhat rough evaluations of the integrals which will arise.

Owing to the term proportional to $c\tau$, the term in φ_2 is normally larger than the rest. As we are only estimating an error it suffices to consider this term alone, i.e. we may choose a model in which

$$(D.2) \quad \begin{cases} \varphi_1 = \varphi_3 = 0 , \\ \varphi_2 = \frac{1}{2} \Omega E_0 (1 + c\tau/\lambda) , \end{cases}$$

typical of our worst cases. To achieve this we have $\partial E_0 / \partial \theta = 0$, whence from Eqs. (3.29) and (2.9) we obtain

$$(D.3) \quad r B_\varphi^{(0)} = \frac{1}{2} \lambda E_0 \Omega \left\{ \left(1 + \frac{c\tau}{\lambda} \right) \frac{k/2\pi\lambda}{1 + k/2\pi\lambda} + \frac{2c\tau}{\lambda} k\sigma \right\} e^{-k\sigma} ,$$

and

$$(D.4) \quad \frac{1}{r^2 \sin \theta} \frac{\partial}{\partial \theta} \left[\sin \theta \cdot r B_\varphi^{(0)} \right] = \frac{\lambda E_0 \Omega'}{2r^2} \left\{ \left(1 + \frac{c\tau}{\lambda} \right) \frac{k/2\pi\lambda}{1 + k/2\pi\lambda} + \frac{2c\tau}{\lambda} k\sigma \right\} e^{-k\sigma} ,$$

where

$$(D.5) \quad \Omega' \stackrel{\text{def}}{=} \frac{1}{\sin \theta} \frac{\partial}{\partial \theta} (\Omega \sin \theta) .$$

In all our cases Ω is of the form $\epsilon \sin \theta$ whence $\Omega' = 2\epsilon \cos \theta$, where ϵ is a small asymmetry factor whose exact form depends on the type of asymmetry under consideration. In all cases, however, $\Omega' \ll 1$. Equation (D.4) gives the source function for the correction $E_r^{(1)}$ to E_r , i.e.

$$(D.6) \quad E_r^{(1)} = e^{-S} \int_0^T \frac{e^S}{r^2 \sin \theta} \frac{\partial}{\partial \theta} (\sin \theta r E_\theta^{(0)}) c d\tau,$$

$$= \frac{\lambda E_0 \Omega'}{2r^2} e^{-k\sigma} \int_0^T \left\{ \left(1 + \frac{c\tau}{\lambda} \right) \frac{k/2\pi\lambda}{1 + k/2\pi\lambda} + \frac{2c\tau}{\lambda} k\sigma \right\} c d\tau.$$

Now the quantity $k/2\pi\lambda$ is always less than unity but is very nearly one for all appreciable values of τ . Similarly, $k\sigma$ is nearly constant for such values of τ and we have

$$(D.7) \quad E_r^{(1)} = \frac{\lambda E_0 \Omega'}{2r^2} e^{-k\sigma} \left[c\tau + \frac{c^2 \tau^2}{2\lambda} (1 + 2k\sigma) \right],$$

to adequate accuracy, and therefore

$$(D.8) \quad \frac{1}{2} \frac{\partial E_r^{(1)}}{\partial \theta} = \frac{\lambda E_0 \Omega'}{4r^2} e^{-k\sigma} \left[c\tau + \frac{c^2 \tau^2}{2\lambda} (1 + 2k\sigma) \right] + O(\epsilon^2).$$

The terms in $O(\epsilon^2)$ vanish identically when $\theta = \pi/2$ and are in general small. We have defined

$$(D.9) \quad \Omega'' = d\Omega'/d\theta.$$

This correction to E_r induces a correction to E_θ which we shall call $E_\theta^{(11)}$. It is given by

$$(D.10) \quad r E_\theta^{(11)} = \int_0^\infty \frac{1}{2} \frac{\partial E_r^{(1)}}{\partial \theta} e^{-X} dr.$$

Setting Eq. (D.8) into (D.10) gives

$$(D.11) \quad r E_\theta^{(11)} = \frac{\lambda E_0 \Omega'}{4} \left[c\tau + \frac{c^2 \tau^2}{2\lambda} \right] \int_0^\infty \frac{e^{-k\sigma - X}}{r^2} dr,$$

plus terms of higher order in (λ/R_s) . Partial integration and the results of Appendix B show that the above integral is simply $1/R_s$ to lowest order and we have

$$(D.12) \quad r E_\theta^{(11)} = \frac{\lambda E_0 \Omega'}{4R_s} \left[c\tau + \frac{c^2 \tau^2}{2\lambda} \right],$$

whereas

$$(D.13) \quad r E_\theta^{(0)} = \frac{\lambda E_0 \Omega}{2} \left[1 + \frac{c\tau}{\lambda} \right] \frac{k/2\pi\lambda}{1 + k/2\pi\lambda}.$$

Clearly the correction term is negligible for small values of τ ; it remains negligible just so long as

$$(D.14) \quad \frac{\Omega'}{2\Omega} \frac{c\tau}{R_s} \ll 1.$$

In addition to $E_\theta^{(11)}$ there is another first-order correction term, $E_\theta^{(12)}$, which has as its source the term

$$(D.15) \quad \sum^{(2)} = \frac{1}{2} \frac{\partial^2}{\partial r^2} \int_0^T r E_\theta^{(0)} c d\tau.$$

This is readily calculated to be

$$(D.16) \quad \sum^{(2)} = \frac{\lambda E_0}{4} \left(c\tau + \frac{c^2 \tau^2}{2\lambda} \right) e^{-k\sigma}$$

$$\left\{ \frac{\partial^2 \Omega}{\partial r^2} + 2k\sigma \frac{\partial(\Omega)}{\partial r} - \Omega^2 [k\sigma - (k\sigma)^2] \right\},$$

and

$$(D.17) \quad r E_\theta^{(12)} = \int_0^\infty \sum^{(2)} e^{-X} dr.$$

When we set Eq. (D.16) into Eq. (D.17), all of the integrals are given in Appendix B except for that

involving the term in $\partial^2 \Omega / \partial r^2$. Writing $\psi = \kappa r + X$, we have

$$(D.18) \quad \int_0^{R_s} e^{-\psi} dr = [re^{-\psi}]_0^{R_s} - \int_0^{R_s} rye^{-\psi} 2\pi\sigma dr,$$

as the result of partial integration. Now using Eq. (B.19) of Appendix B, we obtain

$$(D.19) \quad \int_0^{R_s} e^{-\psi} dr = \gamma \lambda e^{-1},$$

when we make use of the fact that $\psi_s \doteq 1$. Using this result plus others from Appendix B we obtain

$$(D.20) \quad rE_{\theta}^{(12)} = \frac{\lambda^2 E_0 \Omega}{4} \left(c\tau + \frac{c^2 \tau^2}{2\lambda} \right) \left[\gamma e^{-1} \frac{1}{\Omega} \frac{\partial^2 \Omega}{\partial r^2} + \frac{e^{-1} k/2\pi\lambda}{1 + k/2\pi\lambda} \left\{ \frac{\partial z}{\partial r} + \frac{z}{\Omega} \frac{\partial \Omega}{\partial r} \right\} - z^2 \frac{k/2\pi\lambda}{(1 + k/2\pi\lambda)^2} \right]_{r=R_s}.$$

The worst case is that of the atmospheric density gradient for which $\Omega \propto r^2$. Then the term involving

$$(D.21) \quad \frac{z}{\Omega} \frac{\partial \Omega}{\partial r} \doteq \frac{2}{\lambda R_s}$$

dominates the rest and we have

$$(D.22) \quad \frac{E_{\theta}^{(12)}}{E_{\theta}^{(0)}} \approx \frac{c\tau}{eR_s}.$$

From Eqs. (D.14) and (D.22) we can conclude that the high-frequency approximation is valid for all times such that

$$(D.23) \quad c\tau \ll R_s.$$

Note that this conclusion is essentially independent of the magnitude of the secular term.

REFERENCES

1. B. R. Suydam, "Theory of the Radio Flash: Part V, The High Frequency Signal," Los Alamos Scientific Laboratory Report LA-3406-MS (January 1966), Secret RD.
2. B. R. Suydam, "Theory of the Radio Flash: Part VI, High Frequency Signal from a Ground Burst," Los Alamos Scientific Laboratory Report LA-3532-MS (July 1966).
3. C. L. Longmire, "Close-In E.M. Effects, Lectures X and XI," Los Alamos Scientific Laboratory Report LA-3073-MS (April 1964), Secret RD.
4. W. J. Karzas and R. Latter, Phys. Rev. 157, B, 1369 (March 1965).
5. L. W. Miller, "Theoretical Study of the Fast Magnetic Dipole Radio Frequency Signal from Nuclear Explosions," Los Alamos Scientific Laboratory Report LA-3087 (April 1964), Secret RD.
6. L. M. Chanin, A. V. Phelps, and M. A. Biondi, Phys. Rev. 128, 219 (October 1962). See Figs. 5 and 14 of this paper for the field dependence at high field strength; as regards low field strength values, note the relationship between effective electron temperature and applied field as given in Fig. 15.
7. S. Chandrasekhar, Radiation Transfer, Oxford at the Clarendon Press (1950) p. 378.
8. Since this report was written, the signal from differential scattering in the nonuniform atmosphere has been further considered. An estimate of the strength and shape of the signal is given in Los Alamos Scientific Laboratory report LA-4253-MS, by the present author.

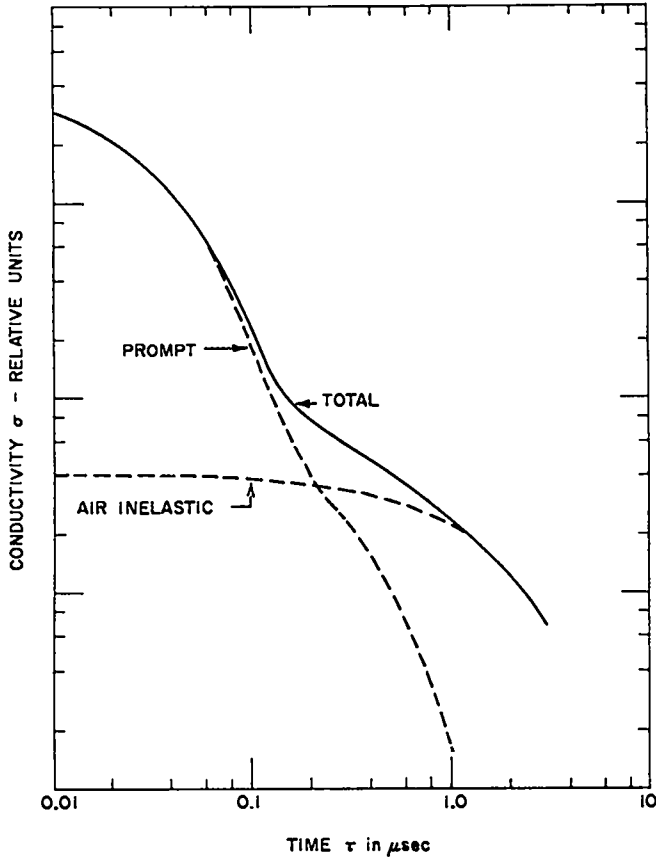


Fig. 1. Typical σ vs. τ history.

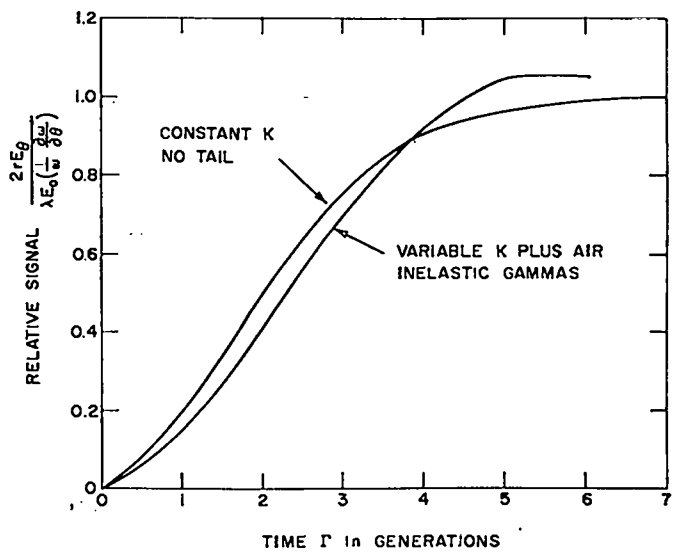


Fig. 3. Bomb asymmetry alone, time in generations.

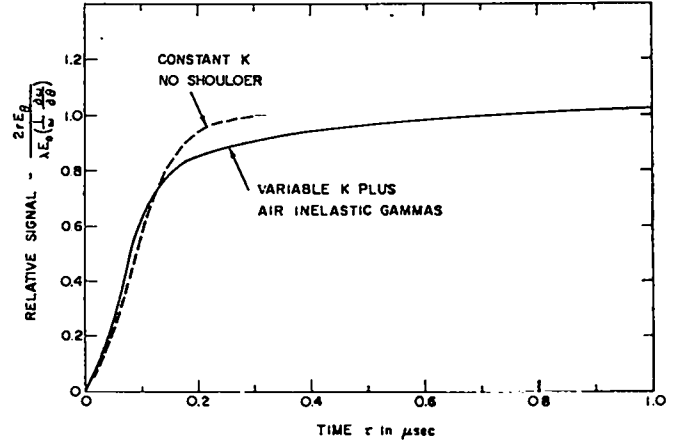


Fig. 4. Bomb asymmetry alone, real time.

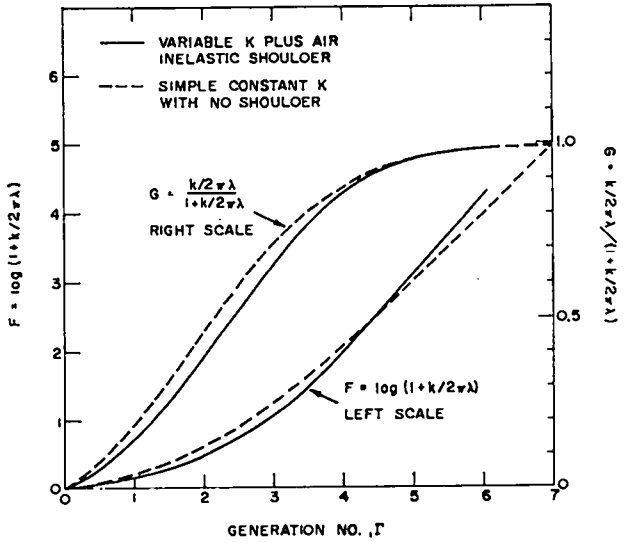


Fig. 2. The "universal" functions F and G.

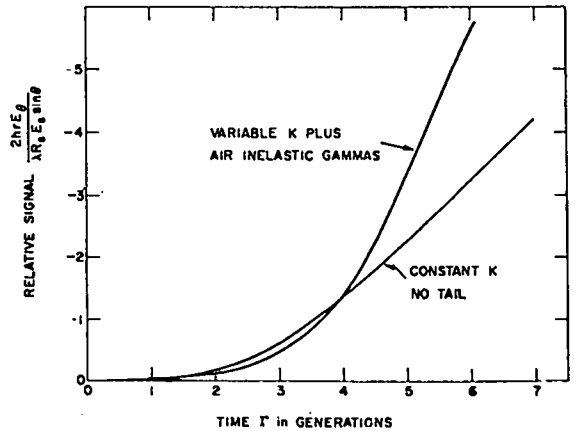


Fig. 5. Water vapor gradient, time in generations.

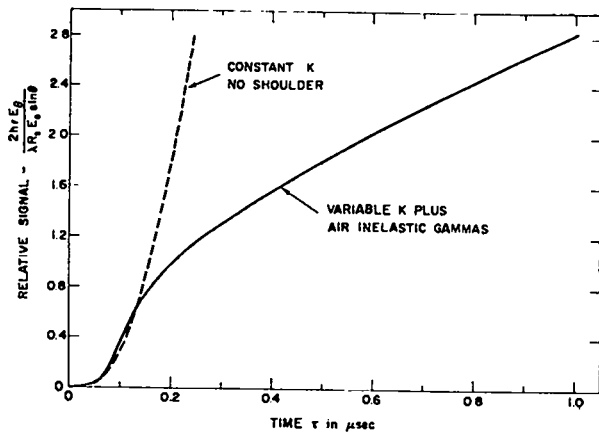


Fig. 6. Water vapor gradient, real time.

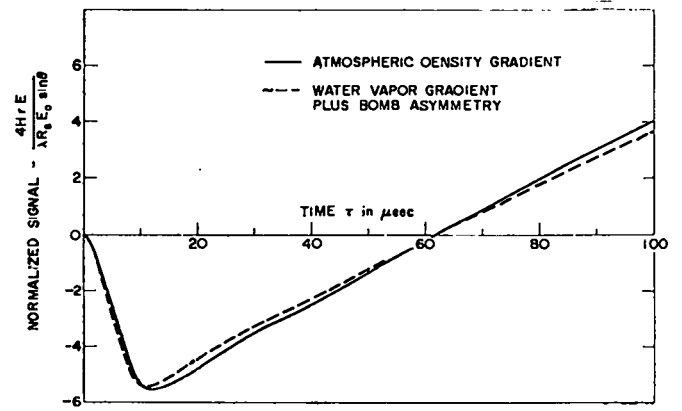


Fig. 9. Linear dependence of the various signals.

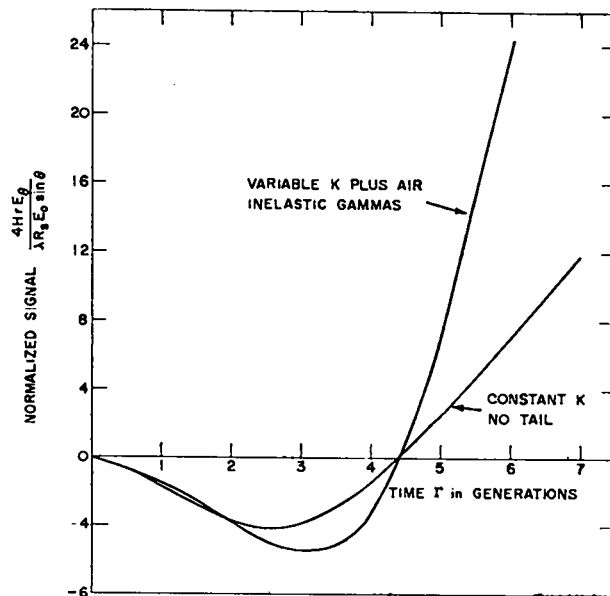


Fig. 7. Atmospheric density gradient, time in generations.

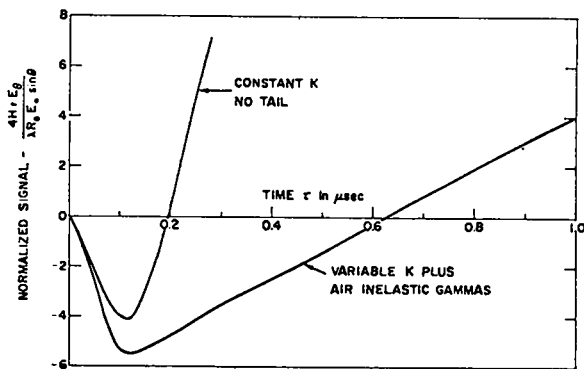


Fig. 8. Atmospheric density gradient, real time.